Catalysis Letters 13 (1992) 247–260

Metal dispersion dependent selectivities for syngas conversion on faujasite X hosted rhodium

A. Martin [1]*, B. Lücke [1], N.J. Jaeger [2], G. Schulz-Ekloff [2], D. Gutschick [1]
and H. Miessner [1]

[1] *Zentrum für Heterogene Katalyse Rudower Chaussee 5, O-1199 Berlin, F.R.G.*
[2] *Institut für Angewandte und Physikalische Chemie Universität Bremen, Bibliothekstr. 2, W-2800 Bremen 33, F.R.G.*

Received 29 November 1991; accepted 24 January 1992

Different metal dispersions of Na-faujasite X hosted rhodium were generated and characterized by transmission electron microscopy (TEM) and IR-spectroscopy. CO hydrogenation has been studied over these Rh/NaX-zeolite catalysts. The finer rhodium dispersion with a mean particle size of 1–2 nm shows a higher selectivity towards oxygenates (methanol, ethanol and dimethyl ether) as compared to the coarser dispersion (4–5 nm), where nearly exclusively methane and higher hydrocarbons are formed.

Keywords: Faujasite X hosted rhodium; rhodium particle size; IR-spectroscopy; TEM; CO hydrogenation

1. Introduction

Rhodium is a catalytically active metal for CO hydrogenation and related reactions like e.g. methanol carbonylation [1–41. The properties of the metal are intermediate between Ir and Pt with respect to the product distribution for the syngas conversion of these catalysts. Jt has been found that the selectivity of methanol formation on Pd, Pt and Ir supported on silica-gel follows the order Pd > Pt > Sr [5]. This order is related to the tendency of the metal to fill its d-shell [6], resulting in the formation of different species in the CO chemisorption.

The catalytic behaviour of rhodium in CO hydrogenation strongly depends on the support used [7–9]. The influence of the metal dispersion on the activity and selectivity of supported catalysts and the problems involved to establish a clear relationship have been thoroughly discussed [10,11]. It is important to note that the metal dispersion may also have primarily an effect on a side reaction rather than on the main reaction thus modifying the catalyst [12,13].

The unambiguous interpretation of particle size effects requires well characterized and distinctly different metal dispersions with narrow particle size distribution. These requirements can be met by using the framework of faujasite type zeolites as hosts for the metal dispersion [14,15].

However, even in the case of such model systems conflicting evidence regarding the effect of the dispersion of Pt and Pd supported on faujasites has been reported for the hydrogenation of CO in [16–18].

According to the results of the CO hydrogenation obtained on faujasite-type zeolite-supported platinum the fine dispersion (1–2 nm) shows a higher methanol selectivity as compared to the coarse one (4–5 nm) [16,17]. The same behaviour has been observed for different particle sizes of zeolite-supported palladium during CO hydrogenation, whereas only low methanol selectivities on either small or large zeolite-supported iridium particles have been found [17].

Based on experience in the preparation of well-defined noble metal/NaX catalysts of Pt, Pd and Ir [14,15,19] the generation of different Rh particle dispersions in NaX zeolite was studied. The extension of this work to different rhodium dispersions encaged in NaX matrices, their characterization, and the selectivity effects of the catalysts in the CO hydrogenation are reported in this paper.

2. Experimental

CATALYST PREPARATION

The catalysts were prepared from iron-free NaX zeolite powder (Si-to-Al ratio of 1.2) by ion exchange from aqueous solutions of $[Rh(NH_3)_5Cl]Cl_2$ (Aldrich) or $[Rh(NH_3)_6](NO_3)_3$ (synthesized according to ref. [20]) at room temperature. The degree of exchange was determined by atomic absorption spectroscopy (AAS) with a Philips PU 9200. The samples were washed with water and dried in air at 353 K. The Rh-complexes were decomposed by temperature-programmed heating (2 K/min) of 1 g of the corresponding sample in a fixed-bed reactor under shallow bed conditions. The samples were heated either under argon (10 l/h, up to 673 K, 5 hours) or oxygen (10 l/h, up to 623 K, overnight). In the case of samples heated under oxygen the reduction was carried out by subsequent treatment with hydrogen (10 l/h, 573 K, 3 hours). The materials investigated, the Rh-compound used for ion exchange, metal loading, reduction treatment and average Rh-particle size are listed in table 1.

CHARACTERIZATION METHODS

The crystallinity of the reduced samples was checked by N_2-physisorption and X-ray diffraction.

Table 1
Materials, treatment, metal loading and surface average diameter d_s of the Rh dispersion

Sample description	Ion-exchange material	Metal loading		Reduction treatment	d_s (nm)
		atom-% [a]	wt.-%		
$RhCl_2/Ar$	$[Rh(NH_3)_5)Cl]Cl_2$	25.7	5.7	heated to 673 K (2 K/min) under Ar, held for 5 hrs	4.6
$RhNO_3/Ar$	$[Rh(NH_3)_6](NO_3)_3$	18.8	4.4		3.9
$RhCl_2/O_2$	$[Rh(NH_3)_5Cl]Cl_2$	25.7	5.7	heated to 623 K (2 K/min) under O_2, held overnight cooling to 573 K under Ar, kept for 3 hrs under H_2 at 573 K	1.3
$RhNO_3/O_2$	$[Rh(NH_3)_6](NO_3)_3$	18.8	4.4		1.4

[a] Exchange degree.

The particle size was determined from transmission electron micrographs obtained on a Philips EM 420 T (LaB_6 filament, 120 kV). The surface average diameter d_s was calculated from the histograms in order to represent the contribution of the particle surface more adequately by using the formula

$$d_s = \sum_i d_i^3 / \sum_i n_i d_i^2 \tag{1}$$

where n_i is the number of crystallites within the diameter d_i and $d_i + \Delta d$ while $d_i = d_i + \Delta d/2$ [21].

IR spectra were recorded in transmission using self-supporting wafers with a diameter of 20 mm and a weight of ca. 7 mg/cm^2. Pretreatment and CO adsorption were performed in situ in a glass cell connected to a vacuum and a gas handling system. Prior to adsorption, the samples, ex situ reduced as described above, were dehydrated at 473 K in vacuo for 30 min. The samples were exposed to ca. 20 Torr CO at 370 K for 10 min and, after evacuation at room temperature (r.t.), the spectra were recorded with a Fourier Transform JR-spectrometer IRF 180 (Zentrum fur wissenschaftlichen Gerätebau/Berlin-Adlershof) at a resolution of 2 cm^{-1}.

The spectra in the range of the skeletal stretching vibrations were obtained by using the KBr wafer technique. 0.5 mg of the sample were ground with 400 mg KBr and pressed at 400 MPa.

APPARATUS AND PROCEDURE FOR THE CO HYDROGENATION

The CO hydrogenation reaction was studied in a continuous plug-flow type reactor (volume 1.57 cm^3). A fluidized bed was established by means of an external vibrator. For the CO hydrogenation reaction the Rh-containing X-zeolite powders were pressed and granulated (grain size 0.4–0.7 mm). The catalyst sample (150 mg) was loaded into the reactor and heated up to 573 K (2 K/min) under argon overnight. CO hydrogenation was performed at 573 K and 2 MPa, a H_2 : CO ratio of 2.33 and a GHSV of 2500 h^{-1} was realized. The effluent stream passed through a heated line to prevent a condensation of the products, wich were analyzed by on-line gas chromatography (Shimadzu GC-9A) equipped with a capillary column (50 m × 0.32 mm i.d., bonded methyl 5% phenylsilicone phase) and a flame ionization detector. Methane, CO and CO_2 were continuously checked by corresponding gas analyzers. The selectivity data given in the tables and figures were expressed as selectivity $S = \{\mathrm{TOF(methanol)/TOF(methane)}\}$ and relative selectivity S_{rel} = (selectivity of fine dispersion/selectivity of coarse dispersion). The ratio of the reaction rates of methanol and methane per catalytic site exposed has been used as a special measure of the selectivity to methanol (S).

3. Results and discussion

CHARACTERIZATION OF ZEOLITE FRAMEWORK (BET, IR)

N_2-physisorption on all reduced samples showed only slightly decreased pore volumes in comparison with the pure NaX-zeolite. According to these data, a significant framework destruction due to the reduction treatment could be excluded. The same conclusion follows from JR spectra in the range of the skeletal stretching vibrations of the zeolite. According to [22] the Si-to-Al ratio of the reduced catalysts can be estimated to be 1.1–1.3.

TRANSMISSION ELECTRON MICROSCOPY (TEM)

Fig. 1 shows a typical bright-field electron micrograph of each of the four rhodium loaded materials after the corresponding reduction treatment as described in table 1. It is clearly seen that the particle size depends on the reduction treatment.

Reduction under inert gas leads to larger particles (4–5 nm), whereas only small crystallites (1–2 nm) have been observed following the oxygen treatment and subsequent hydrogen reduction.

The histograms of the metal dispersions depicted in fig. 2 for samples $RhCl_2/Ar$ and $RhCl_2/O_2$ and in fig. 3 for samples $RhNO_3/Ar$ and $RhNO_3/O_2$ were evaluated from the electron micrographs shown in fig. 1. The distribution is given for the size, the corresponding metal mass and metal surface contribution of the particles.

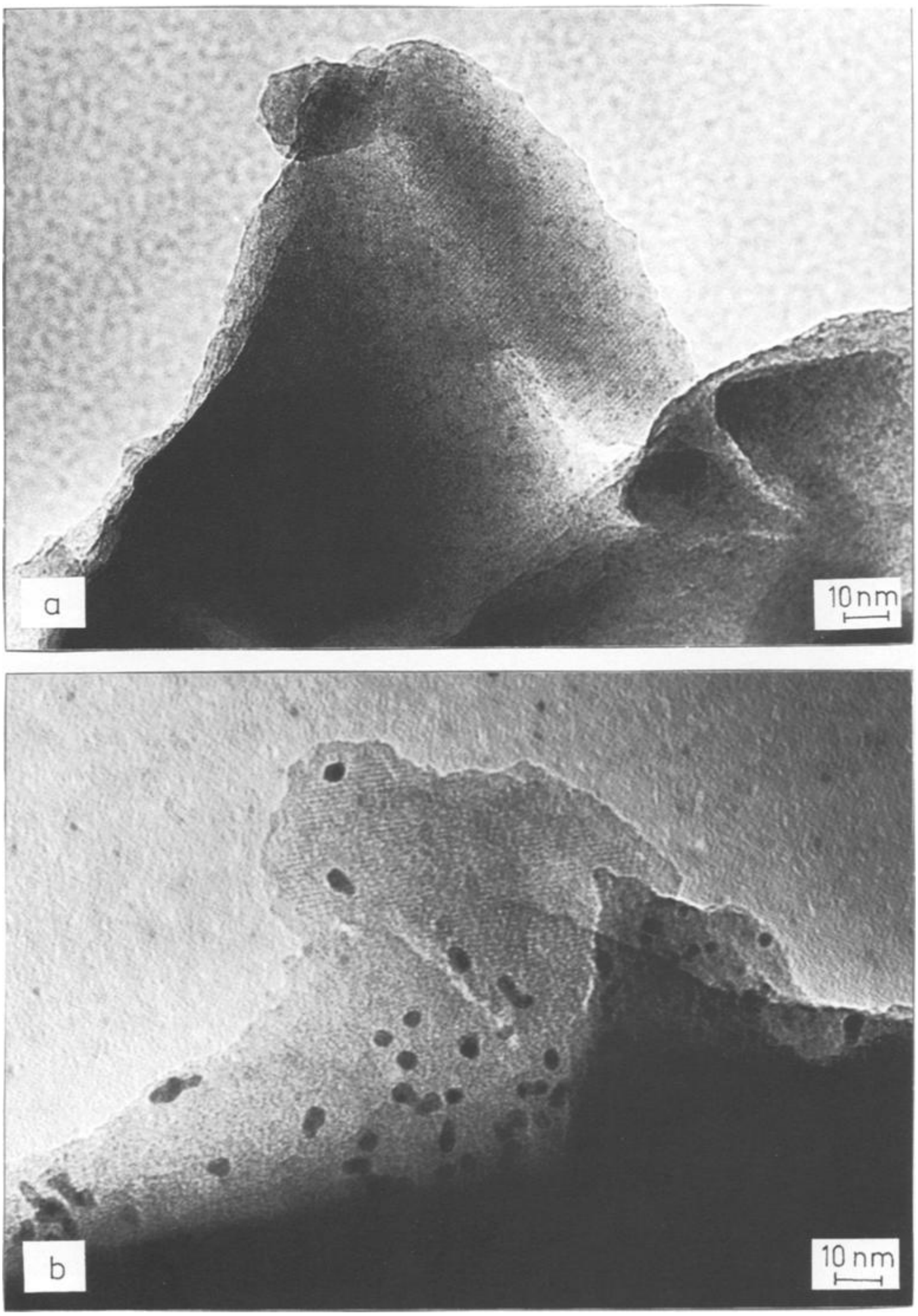

Fig. 1. Electron micrographs of the Rh/NaX specimen after reduction treatment; (a) $RhCl_2/O_2$, (b) $RhCl_2/Ar$, (c) $RhNO_3/O_2$, (d) $RhNO_3/Ar$.

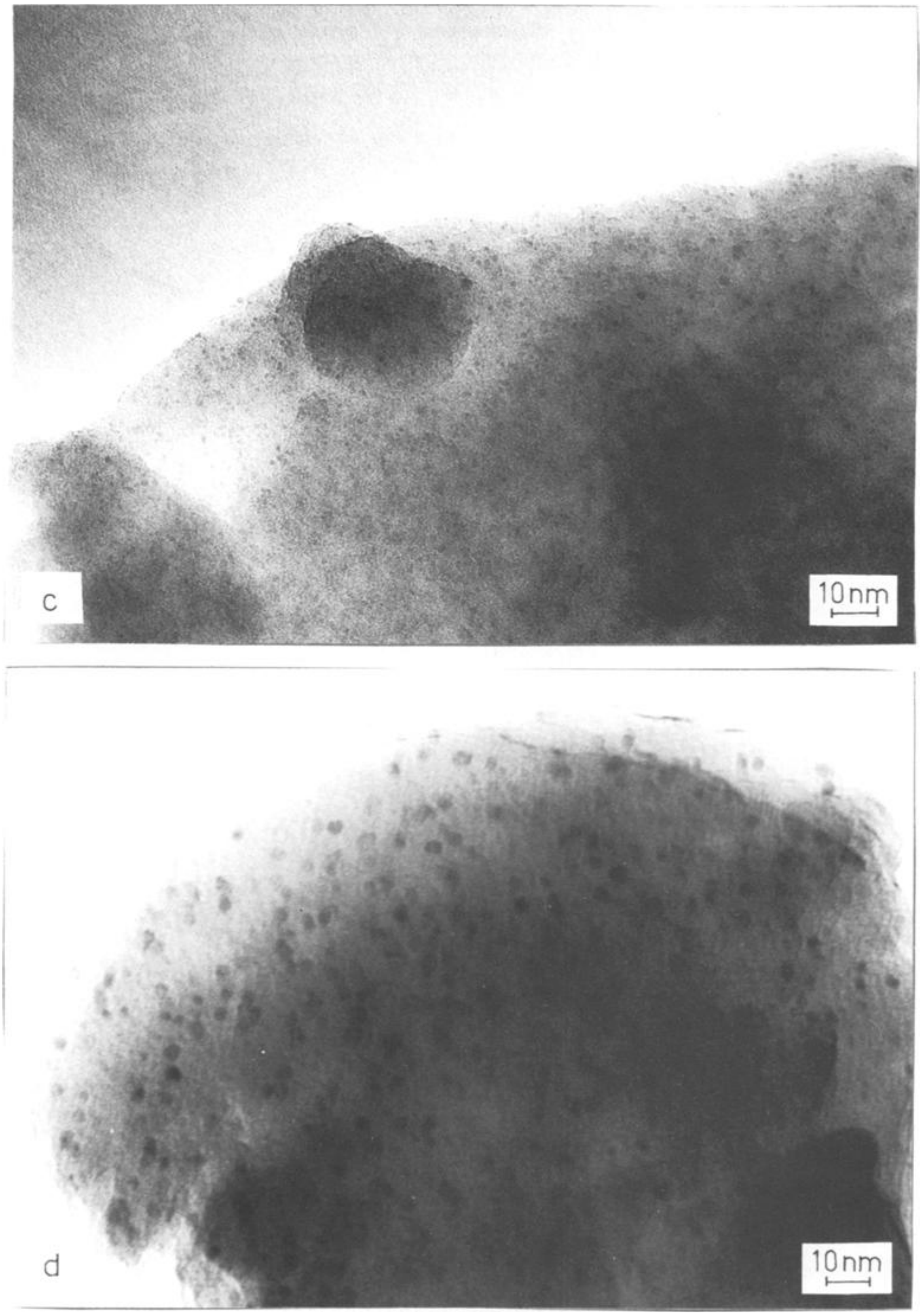

Fig. 1. (continued).

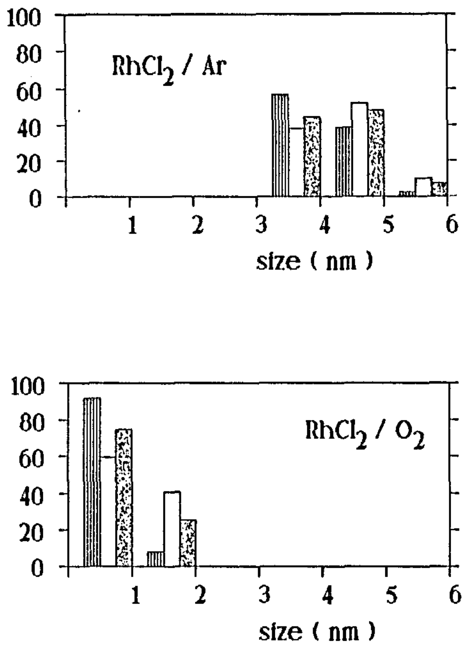

Fig. 2. Particle size distribution of $RhCl_2/Ar$ and $RhCl_2/O_2$. The bars represent integer numbers. ▥ particle %; ☐ mass %; ▨ surface %.

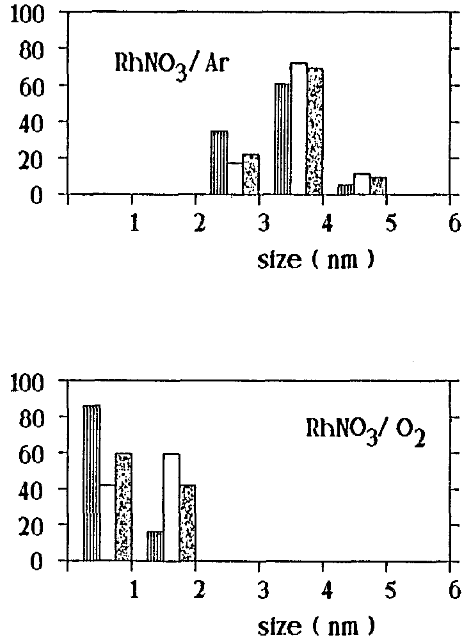

Fig. 3. Particle size distribution of $RhNO_3/Ar$ and $RhNO_3/O_2$. The bars represent integer numbers. ▥ particle %; ☐ mass %; ▨ surface %.

FOURIER-TRANSFORM INFRARED SPECTROSCOPY (FTIR) OF ADSORBED CO

It is well known that different species of adsorbed CO on dispersed Rh can be formed [23]. In addition to the linearly adsorbed and the bridge-bonded CO on metallic Rh sites the gem-dicarbonyl Rh(I)$(CO)_2$ is formed, especially on higly dispersed Rh. According to Van't Blik et al. [24] the formation of Rh(I)$(CO)_2$ with Rh in the oxidation state +1 proceeds by disruption of Rh-Rh bonds followed by an oxidation of the isolated Rh-atoms. Therefore, CO can be used as a probe molecule to distinguish between Rh catalysts of different dispersion. The IR spectra of CO adsorbed on the different catalysts are shown in fig. 4. In the case of the catalysts first treated with oxygen and finally reduced with hydrogen two absorption bands at 2015 and 2098 cm^{-1} can be assigned to the Rh(I)$(CO)_2$ species. The intensity of the bands depends on the precursor used for the preparation and was found to be around five times higher for $RhCl_2/O_2$ (curve a) as compared to $RhNO_3/O_2$ (curve b). The reason is not yet understood. A possible explanation could be that the reduction of the $RhCl_2$-derived catalysts to metallic Rh is not complete due to stabilization of Rh^{1+} by coordinated chlorine. This means that the formation of the gem-dicarbonyl does not only proceed by disruption of Rh atoms from the metal crystallites but also by carbonylation of Rh^{1+} species. Jn the case of the $RhNO_3/O_2$ sample the reduction to metallic rhodium should be complete. A very small and broad absorption between 1800–1900 cm^{-1} for $RhCl_2/O_2$ points to the presence of a small amount of bridge-bonded CO. The absorption of the linear bonded CO on Rh^0 which should be expected between the two bands of the dicarbonyl may be masked by the intense twin band.

Both catalysts treated in argon show the twin band at 2015 and 2098 cm^{-1}, too, but with significantly lower intensity, indicating the presence of larger rhodium crystallites. Possibly remaining amounts of cationic rhodium in the sample $RhNO_3/Ar$ should be rather small because the intensity of the twin band is ca. five times lower than for the sample $RhNO_3/O_2$ (note the different scales in fig. 4). The broad absorption near 1850 cm^{-1} (curves c and d) due to bridge-bonded CO is much more pronounced than for the samples treated in O_2 and reduced with H_2, which is also an indication of the presence of larger rhodium crystallites.

These results are in good agreement with the electron micrographs. The higher dispersed particles form mainly Rh(I)dicarbonyl species by interaction with CO, whereas bridge-bonded CO is present in remarkable amounts on the less dispersed particles.

CATALYTIC STUDIES

The CO hydrogenation results show several significant features. The major products observed are methane, C_2-C_4 hydrocarbons and methanol. Ethanol

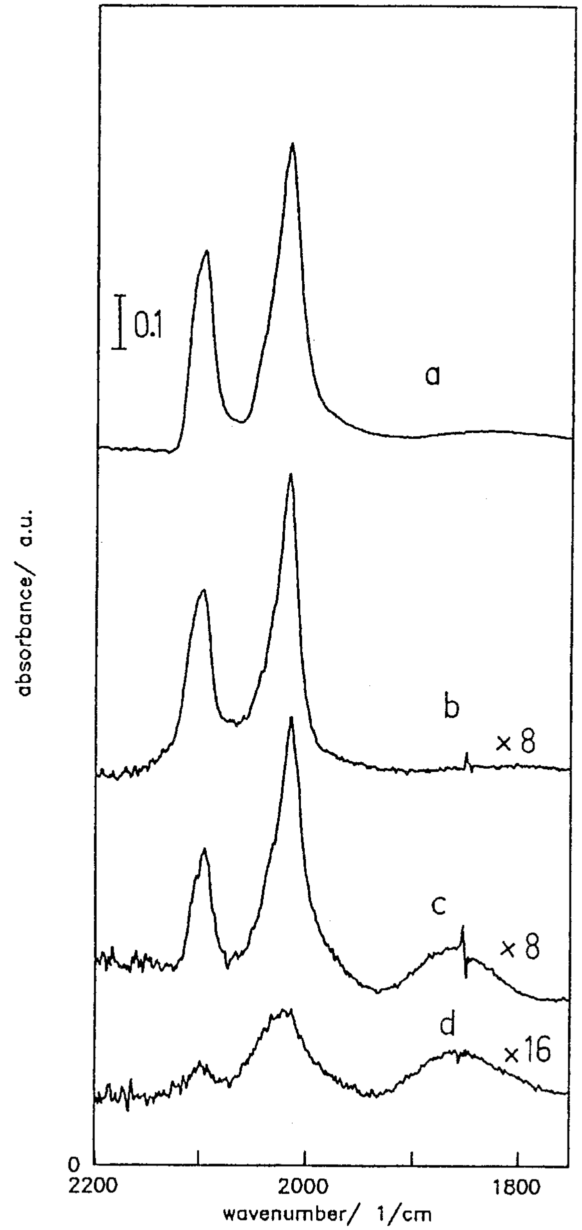

Fig. 4. FTIR spectra of adsorbed CO on (a) $RhCl_2/O_2$, (b) $RhNO_3/O_2$, (c) $RhCl_2/Ar$, and (d) $RhNO_3/Ar$. (Note the changed intensity scale.)

and dimethyl ether are obtained in minor amounts and for the fine dispersion only.

Figs. 5 and 6 depict the selectivity-relations $S = \{\text{TOF (methanol)}/\text{TOF(methane)}\}$ in dependence of time on-stream of $RhCl_2/O_2$, $RhCl_2/Ar$ and

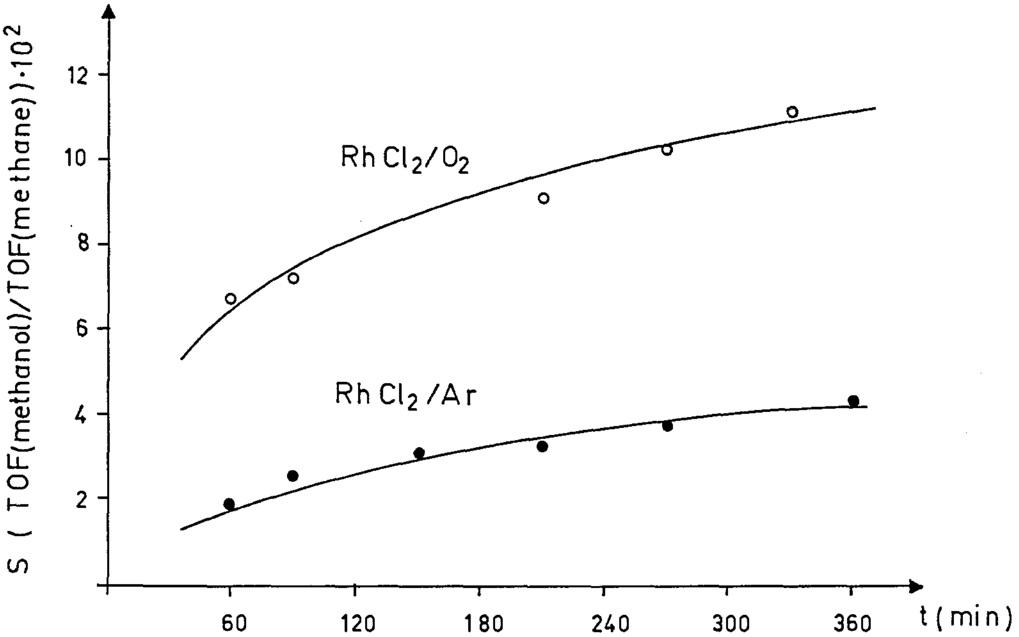

Fig. 5. Selectivities S of CO hydrogenation on $RhCl_2$ samples (fine and coarse dispersion) during time on-stream (573 K, 2 MPa, $H_2:CO = 2.33$, 2500 h^{-1}).

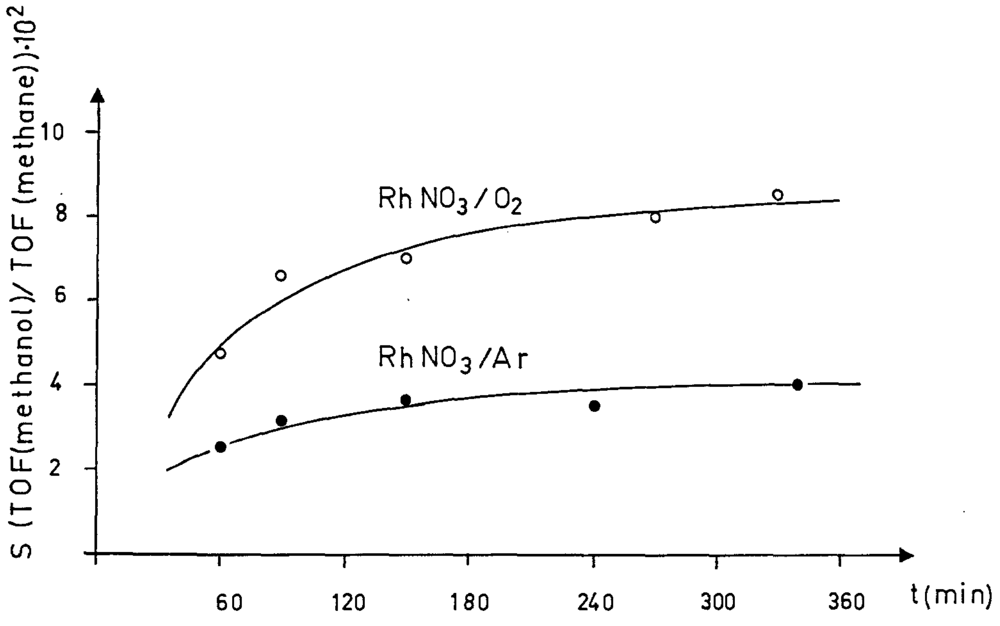

Fig. 6. Selectivities S of CO hydrogenation on $RhNO_3$ samples (fine and coarse dispersion) during time on-stream (573 K, 2 MPa, $H_2:CO = 2.33$, 2500 h^{-1}).

$RhNO_3/O_2$, $RhNO_3/Ar$ catalysts, respectively. It is clearly shown that the selectivity for the formation of oxygenates, mainly methanol, on catalysts containing smaller Rh particles is higher than on that with the larger ones. The formation of methanol proceeds with molecularly adsorbed CO, whereas hydrocarbons are formed via CO dissociation. The CO dissociation needs a fairly large ensemble of metal atoms [25] and should be favored on large Rh crystallites.

It should be noted that the NaX support contains a high amount of Na^+-ions, which are known to influence the oxygenate selectivity in CO hydrogenation on Rh-containing catalysts. The influence of particle size on the interaction between metal particles and K^+-ions has been shown for the IR spectra of CO adsorbed on Pd/SiO_2 [26]. A shift of the stretching vibration of CO adsorbed on supercage sized Pt in NaX to lower frequencies at low pressures and higher temperatures has also been attributed to the interaction with Na^+-ions [27]. However, whether this interaction is present in our Rh/NaX systems and/or has any influence on the hydrogenation of CO cannot be assessed at the present time.

Furthermore, during time on-stream a distinct formation period can be observed. With increasing reaction time the selectivity to oxygenates increases on all catalyst samples and dispersions accompanied by a decrease of the overall activity (fig. 7). The reason for this behaviour may be found in the formation of coke on the catalyst surface [17]. The coke formation causes a decrease of the

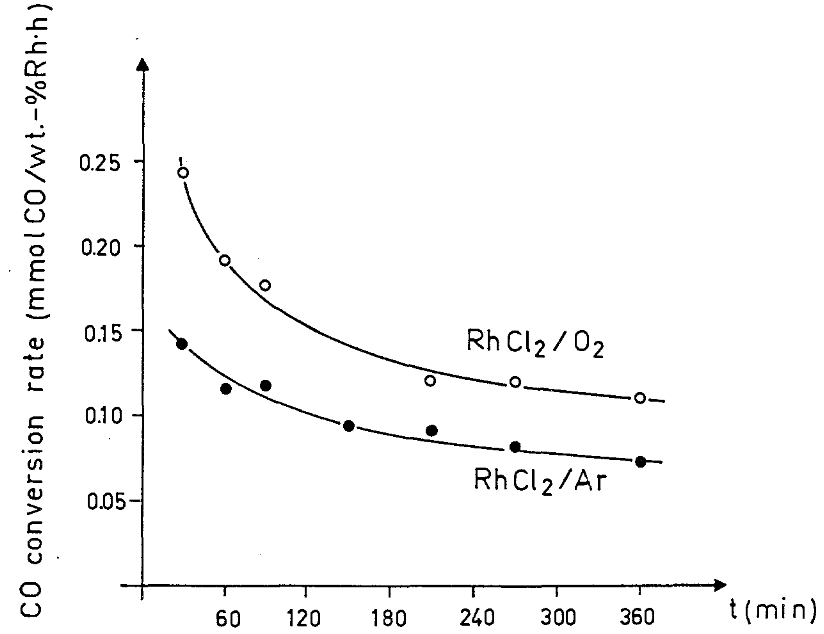

Fig. 7. Rate of CO conversion on $RhCl_2$ samples (fine and coarse dispersion) during time on-stream (573 K, 2 MPa, $H_2:CO = 2.33$, 2500 h^{-1}).

Table 2
Selectivities $S = \{\mathrm{TOF\ (methanol)}/\mathrm{TOF\ (methane)}\}$ and relative selectivities S_{rel} = (selectivity of fine dispersion/selectivity of coarse dispersion) in CO hydrogenation at 573 K, after 300 min time on-stream, 2 MPa, $H_2:CO = 2.33$ and 2500 h^{-1}

Sample	d_s (nm)	$S * 10^2$	S_{rel}
$RhCl_2/Ar$	4.6	4.0	2.7
$RhCl_2/O_2$	1.3	10.7	
$RhNO_3/Ar$	3.9	4.0	2.1
$RhNO_3/O_2$	1.4	8.3	

number of active sites leading to a decreased activity. At the same time the density of large metal ensembles responsible for the CO dissociation might decrease resulting in the enhanced selectivity to oxygenates with time on-stream.

Table 2 lists the selectivities S and the relative selectivities S_{rel} = (selectivity of fine dispersion/ selectivity of coarse dispersion) after 300 min on-stream. For the relative selectivity of $RhCl_2$ and $RhNO_3$ sample values of 2.7 and 2.1, respectively, are obtained. Comparing these with results obtained in the CO hydrogenation on analogously prepared Pt-, Pd- and Ir-zeolite supported (NaX) catalysts [16,17] the following order for the relative selectivity can be established:

$$\mathrm{Pt} > \mathrm{Pd} > \mathrm{Rh} > \mathrm{Ir} \tag{2}$$

Summing up this section, during the CO hydrogenation the selectivity to oxygenates, mainly methanol, is higher on smaller Rh crystallites. The selectivity increases, and the overall activity decreases with time on-stream on smaller as well as on larger Rh particles. The coke formation and particularly, the nature of the coke and its influence on the catalytic selectivity need further investigation.

Acknowledgements

We thank Mr. A. Tonscheidt for taking the electron micrographs and Mr. H. Kompa for carrying out the N_2-physisorption measurements. Financial support by the Bundesminister für Forschung und Technologie (BMFT 423-4003-03C258 3) is gratefully acknowledged.

References

[1] M. Ichikawa, T. Fukushima and K. Shikakura, *Proc. VIIIth Int. Congr. Catalysis*, Berlin (West) (Verlag Chemie, Weinheim, 1984) Vol. II, p. 69.

[2] M. Ichikawa, J. Chem. Soc., Chem. Commun. (1978) 566.
[3] T. Iizuka, Y. Tanaka and K. Tanabe, J. Catal. 76 (1982) 1.
[4] H. Miessner, H. Ewald, D. Gutschick, H. Müller and B. Lücke, Z. Phys. Chem., Leipzig, 271 (1990) 1103.
[5] M.L. Poutsma, L.F. Elek, P.A. Ibarbia, A.P. Risch and J.A. Rabo, J. Catal. 52 (1978) 157.
[6] K. Klier in: *Catalysis of Organic Reactions*, ed. W.P. Moser (Marcel Dekker Inc., New York, 1981) p. 195.
[7] G. van der Lee, Ph. D. Thesis, Leiden, 1986.
[8] T.J. Lee and B.C. Gates, Catal. Lett. 8 (1991) 15.
[9] M. Ichikawa, Bull. Chem. Soc. Jpn. 51 (1978) 2268.
[10] J.R. Anderson, Sci. Prog. (Oxford) 69 (1985) 461.
[11] M. Che and C.O. Bennett, Adv. Catal. 36 (1989) 55.
[12] J.G. van Senden, E.H. van Broekhoven, C.T.J. Wreesman and V. Ponec, J. Catal. 87 (1984) 468.
[13] E.H. van Broekhoven, J.W.F.M. Schoonhoven and V. Ponec, Surf. Sci. 156 (1985) 899.
[14] P. Gallezot, A. Alarcon-Diaz, J.A. Dalmon, A.J. Renouprez and B. Imelik, J. Catal. 39 (1975) 334.
[15] A. Kleine, P.L. Ryder, N.I. Jaeger and G. Schulz-Ekloff, J. Chem. Soc., Faraday Trans. 1, 82 (1986) 205.
[16] N.I. Jaeger, G. Schulz-Ekloff and A. Svensson in: *Proc. VIIth Int. Zeolite Conf.* Tokyo 1986, eds. Y. Murakami, A. Iijima and J.W. Ward (Kodansha, Tokyo - Elsevier, Amsterdam, Oxford, New York, Tokyo, 1986) p. 923.
[17] N.I. Jaeger, G. Schulz-Ekloff and A. Svensson, in: *Studies in Surface Science and Catalysis*, Vol. 65, *Catalysis and Adsorption by Zeolites*, eds. G. Öhlmann, H. Pfeiffer and R. Fricke (Elsevier, Amsterdam, 1991) p. 327.
[18] F.A.P. Cavalcanti, C. Dossi, L.L. Sheu and W.M.H. Sachtler, Catal. Lett. 6 (1990) 289.
[19] D. Exner, N.I. Jaeger, A. Kleine and G. Schulz-Ekloff, J. Chem. Soc., Faraday Trans. 1, 84 (1988) 4097.
[20] S.M. Jörgensen, J. prakt. Chem. 44 (1891) 48.
[21] N.I. Jaeger, A. Jourdan and G. Schulz-Ekloff, J. Chem. Soc., Faraday Trans. 87 (1991) 1251.
[22] H. Fichtner-Schmittler, U. Lohse, H. Miessner and H.-E. Maneck, Z. Phys. Chem., Leipzig, 271 (1990) 69.
[23] H. Miessner, D. Gutschick, H. Ewald and H. Müller, J. Mol. Catal. 36 (1986) 359; and references therein.
[24] H.F.J. Van't Blik, J.B.A.D. Van Zon, T. Huizinga, J.C. Vis, D.C. Koningsberger and R. Prins, J. Phys. Chem. 87 (1983) 2264.
[25] W.M.H. Sachtler and M. Ichikawa, J. Phys. Chem. 90 (1986) 4752.
[26] P.A.J.M. Angevaare, H.A.C.M. Hendrickx and V. Ponec, J. Catal. 110 (1988) 11.
[27] H. Bischoff, Ph. D. Thesis, Bremen, 1991.